Antarct. Meteorite Res., **13**, 65–77, 2000

On the relationship between troilite and/or magnetite rimmed FeNi metals and subtype in CO3 chondrites

Naoya Imae and Hideyasu Kojima

Antarctic Meteorite Research Center, National Institute of Polar Research, Kaga 1-chome, Itabashi-ku, Tokyo 173–8515

Abstract: A lot of troilite and/or magnetite rimmed FeNi metal grains have been found in 22 CO3 chondrites. The morphology of these grains is the most characteristic in opaque mineral assemblages in CO3s. These could be formed by reactions of FeNi metals with S-rich and/or O-rich gas. The number density of rimmed FeNi metals are correlated with subtype of CO3s. The grain size and the rim thickness of these grains are not significantly correlated with subtype. Magnetite is dominantly found in lower subtype (< 3.2) and troilite is abundant but magnetite does not occur except Isna (3.6) and Ornans (3.3) in higher subtype (> 3.2). In the subtype less than 3.2, troilite as inner rim and magnetite as outer rim could coexist for some rimmed FeNi metals (ALH-77307 and Y-81020). These textural variations were not formed by one series of thermal metamorphism but formed by (1) the differences of O/S conditions at the time of thermal metamorphism on the parent body, (2) oxidation from intermediate subtype to lower type and sulfidation from intermediate subtype to higher subtype, or (3) thermal metamorphism of rimmed FeNi metals especially in chondrules enclosed in mafic silicates at lower subtype formed in the solar nebula.

1. Introduction

A lot of troilite and/or magnetite rimmed FeNi metals have been found from unequilibrated chondrites (*e.g.*, Rubin, 1991; Imae, 1994). In some ordinary chondrites, metal accompanies carbides rim (Krot *et al.*, 1997; Krot and Todd, 1998). Allende (CV3) includes abundant magnetite rimmed FeNi metal grains (*e.g.*, Rubin, 1989; Haggerty and McMahon, 1979), ALH-764 (LL3.2/3.4 breccia) and Y-791717 (CO3.2) troilite rimmed FeNi metal grains (Imae, 1994; Lauretta *et al.*, 1996a), and Semarkona (LL3.0) troilite rimmed FeNi metal grains (Rubin *et al.*, 1999). Immiscibility of metal and magnetite has been proposed for the petrogenesis of magnetite rimmed FeNi metals in Allende (Haggerty and McMahon, 1979). While, the assemblages could be formed by metal-gas reaction (*e.g.*, Rubin, 1991; Imae, 1994; Lauretta *et al.*, 1996a; Rubin *et al.*, 1999). Two layer structure, dividing the rim into inner and outer, seen in sulfide or magnetite rimmed FeNi metals in some unequilibrated chondrites suggest the petrogenesis of metal-gas reaction rather than the immiscibility since the experiments of metal-gas reaction have reproduced the texture (Imae, 1994; Lauretta *et al.*, 1996b, 1997).

Metal grains in a lot of unequilibrated chondrites have thus experienced sulfidation, oxidation and carbidization.

Shibata and Mastueda (1994) and Shibata (1996) have studied opaque mineral assemblages in CO3s (Y-74135, -790992, -791717, -81020, -81025, -82050, -82094, and ALH-77307). Shibata (1996) has found cohenite in the least petrologic subtype CO3s. Studies of opaque minerals in CO3s have been limited. We have found that both troilite and/or magnetite rimmed FeNi metal grains are especially rich in CO3. CO3s have experienced thermal metamorphism, and metamorphic sequence (subtype) has been proposed (McSween, 1977; Scott and Jones, 1990; Kojima *et al*, 1995). Rubin (1989) has discussed that there is a relationship between chondrule size and metamorphic sequence in CO3; when metamorphism proceeds, chondrule size tends to become larger. While, more recently, Rubin (1998) described that the correlation between chondrule size (and the other features) and metamorphism may be an artifact resulting from the obliteration of small chondrules during metamorphism. It has not been examined whether there is some relationship between the grain size and/or rim thickness of rimmed FeNi metals, and the metamorphic sequence or not. Since opaque minerals must be more sensitive to the temperature change than silicates, the grain size and rim thickness of rimmed FeNi metals, and the mineral assemblages might become a better indicator of metamorphism.

Then we studied CO3s in order to clarify the general relationship between rimmed FeNi metals and the metamorphic sequence (subtype).

2. Experiments

We examined polished thin sections (PTSs) of 20 CO3 chondrites including two nonantarctic meteorites in National Institute of Polar Research (NIPR) and 2 CO3s in U. S. National Museum of Natural History in Smithsonian Institution (USNM) using an optical microscope and a SEM with EPMA (JXA-733 and JXA-8800). Studied 22 CO3s are ALH-77003, ALH-77307, Y-791131, Y-791433, Y-791717, Y-791745, Y-791746, Y-791748, Y-794088, Y-81002, Y-81020, Y-81067, Y-81068, Y-82004, Y-82050, Y-82094, Y-8339, Lance, Isna and Colony in NIPR and are Ornans and Kainsaz in Smithsonian Institution (Table 1). The group of Y-791745, -1746, and -1748 or the group of Y-81067 and -068 may be paired judging from the proximity of the occurrence in Yamato bare ice field.

Random analyses of olivine grains > about 5 μm in size to determine subtype were carried out by electron probe microanalyzer (EPMA) (JEOL JXA-733). Analyses of opaque minerals and the silicate minerals except the purpose of random analyses were done by EPMA (JEOL JXA-8800).

We measured the grain diameter and the rim thickness under the optical microscope from one PTS (about 0.2–1 cm^2). We defined the diameter as the average of the maximum size and the minimum size and the thickness as the average of the maximum thickness and the minimum thickness. Whether the iron-oxide occurs or not in one PTS was determined under the optical microscope. The iron-oxide phase was identified by EPMA. Corrosion texture of opaque minerals

Table 1. Studied 22 CO3 samples.

Name	Abbreviation	Source	PTS No.
ALH-77003	A	NIPR*[1)]	89-2
ALH-77307	B	NIPR	85-1
Y-791131	C	NIPR	51-1
Y-791433	D	NIPR	51-1
Y-791717	E	NIPR	62-5
Y-791745	F	NIPR	51-1
Y-791746	G	NIPR	51-1
Y-791748	H	NIPR	51-2
Y-794088	I	NIPR	51-1
Y-81002	J	NIPR	51-1
Y-81020	K	NIPR	56
Y-81067	L	NIPR	51-1
Y-81068	M	NIPR	51-1
Y-82004	N	NIPR	51-1
Y-82050	O	NIPR	101-2
Y-82094	P	NIPR	91-1
Y-8339	Q	NIPR	51-1
Lance	R	NIPR	50-1
Isna	S	NIPR	20-1
Colony	T	NIPR	51-1
Ornans	U	USNM*[2)]	1105-5
Kainsaz	V	USNM	2486-9

*[1)] National Institute of Polar Research.
*[1)] U.S. National Museum of Natural History, Smithsonian Institution.

due to Antarctic weathering was excluded for the present study. The distinction between troilite and magnetite was not made in measuring the rim thickness since both can coexist as rim in one grain, but we checked whether magnetite is present in the PTSs (the last column on Table 2).

3. Results

Troilite and/or magnetite rimmed FeNi metals commonly occur in all samples of available 22 CO3s by the observation of PTSs (Fig. 1 and Table 2). Paragenesis of these metals can be divided into two: in chondrule (Fig. 1a) and in matrices (Fig. 1b and c). The rimmed FeNi metals in matrices are larger than those in chondrules. The number density of these metals in matrices is smaller than that in chondrules. Magnetite rimmed metals in chodrules dominantly occur in lower petrologic subtype less than 3.2 (Fig. 1a). The shape of magnetite rimmed metals in chondrules is rounded. On the other hand the shape of rimmed metals in matrix is irregular. Rimmed metals in chondrules are rare in higher petrologic subtype more than 3.2. Troilite rimmed metals are dominant at higher petrologic subtype more than 3.2 (Fig. 1c). In some cases (less than 3.2), mixed rims of troilite and magnetite occur (ALH-77307 and Y-81020) (Fig. 1b). In rimmed FeNi metals for which magnetite

Table 2. Results.

Name	Surface area (mm²)	Measured number of rimmed FeNi	Subtype					Mt*3)
			Fa (mol%)	Fa*1)	Fa*2)	TL*2)	Rec.*2)	
ALH-77003,89-2	56	22	18.8	3.4	3.5		3.4	–*3)
ALH-77307,85-1	41	81	8.9	3.0	3.2	3.2	3.1	+*3)
Y-791131,51-1	26	6	18.1	3.3				–
Y-791433,51-1	24	4	19.5	3.4				–
Y-791717,62-5	172	10	14.6	3.2				–
Y-791745,51-1	47	15	15.2	3.2				–
Y-791746,51-1	33	7	15.2	3.2				–
Y-791748,51-2	21	30	9.5	3.0				–
Y-794088,51-1	29	22	13.0	3.1				+
Y-81002,51-1	20	15	7.1	3.0				+
Y-81020,56	89	17	11.6	3.1				+
Y-81067,51-1	51	69	14.2	3.2				+
Y-81068,51-1	15	20	7.8	3.0				+
Y-82004,51-1	19	17	12.0	3.1				+
Y-82050,101-2	3	4	15.0	3.2				–
Y-82094,91-1	130	16	1.7	3.0	××	3.5	3.5	–
Y-8339,51-1	14	23	12.0	3.1				+
Lance,50-1	51	15	12.9	3.1	3.5	3.4	3.4	+ (minor)
Isna,20-1	74	3	27.0	3.6	3.8	3.8	3.7	+ (minor)
Colony,51-1	61	0	3.9	3.1	3.2	3.0	3.0	(+)*4)
Ornans,1105-5	33	37	16.0	3.3	3.4	3.4	3.4	+
Kainsaz,2486-9	96	31	13.1	3.1	3.1	3.5	3.2	–

*1) Based on the mean fayalite contents determined in the present study according to the definition by Scott and Jones (1990).
*2) Subtype from mean fayalite (Fa), thermoluminescence (TL), and recommendation (Rec.) by Sears *et al.* (1991).
*3) Mt = magnetite, – shows magnetite absent, + shows magnetite appearing.
*4) Weathered.

and troilite coexist, inner rim is troilite and outer rim is magnetite (Fig. 1a in this paper and Fig. 6 in Shibata, 1996).

The number of measurable grains was limited to be from a few to about 80 per one PTS (Table 2). The measured grain diameter is the range of 20–180 μm in average, and the measured rim thickness is the range of 4–50 μm in average for 22 CO3s. The measured diameter and the measured rim thickness are positively correlated (Fig. 2).

The mean fayalite contents of 22 CO3s were determined by random analyses using an electron microprobe analyzer (Table 2). Each chondrite was assigned a subtype based on the mean fayalite content and the criteria of Sears *et al.* (1991).

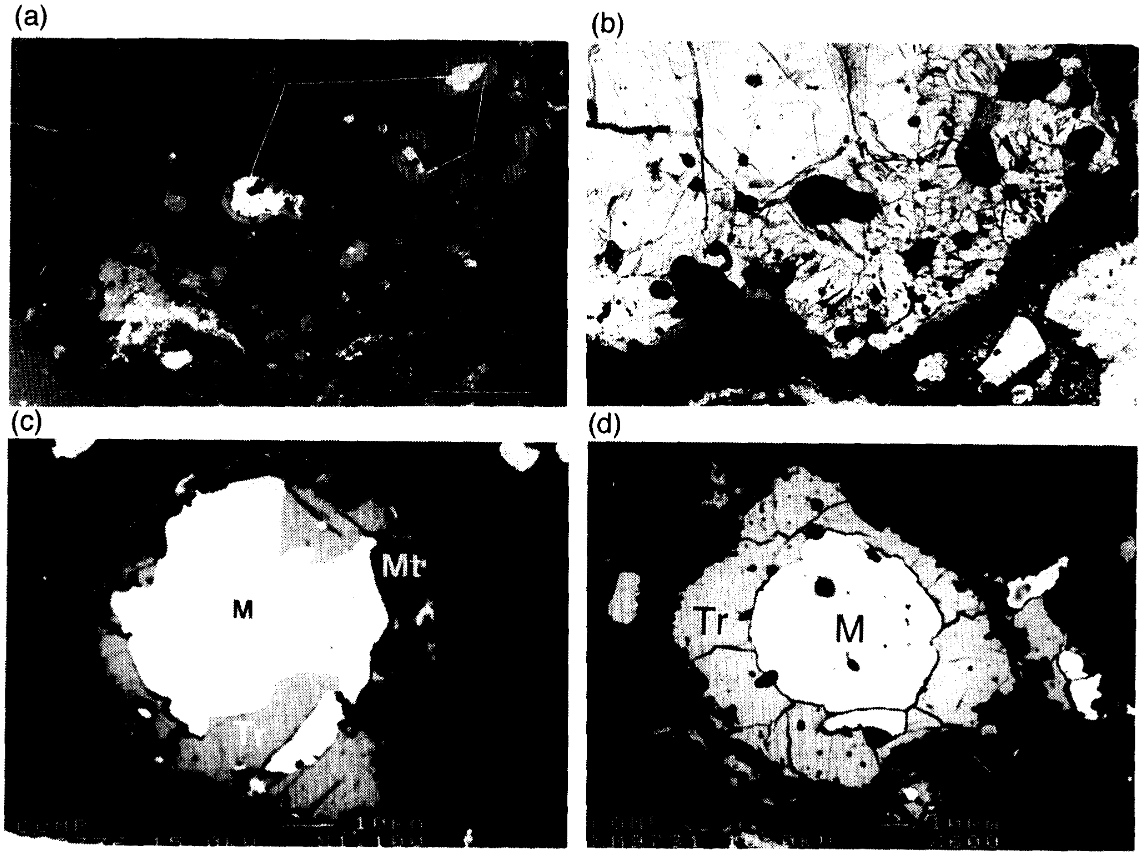

Fig. 1. Images of representative rimmed FeNi metals. M=FeNi metal. Tr=troilite. Mgt= magnetite. (a) Magnetite rimmed FeNi metals in chondrule (Y-81002). Under optical microscope (reflected light). Scale bar corresponds to 75 μm. (b) Image under optical microscope (reflected light) of (a). (c) Troilite and magnetite rimmed FeNi metal in matrix (Y-81020). Back scattered electron image. (d) Troilite rimmed FeNi metal in matrix (Y-791717). Back scattered electron image.

4. Discussion

4.1. The relationship between size and thickness

The apparent diameter (D) and rim thickness (d) are positively correlated (Fig. 2). However, to test whether the real values of these parameters are correlated we consider the effects of observing in sections.

We therefore take into consideration the effect of the cross section of grains, when we observe thin sections, in order to obtain the real distribution of the grain size and the rim thickness (*e.g.*, Hughes, 1978; Eisenhour, 1996). For the simplest case, we consider the cross section of a constant sphere with a constant rim thickness. Then the apparent rim thickness and grain diameter would be related by the eq. (1),

$$d=\frac{D}{2}-\sqrt{\frac{D^2}{4}-D_{\mathrm{real}}\cdot d_{\mathrm{real}}+d_{\mathrm{real}}^2}\,, \qquad (1)$$

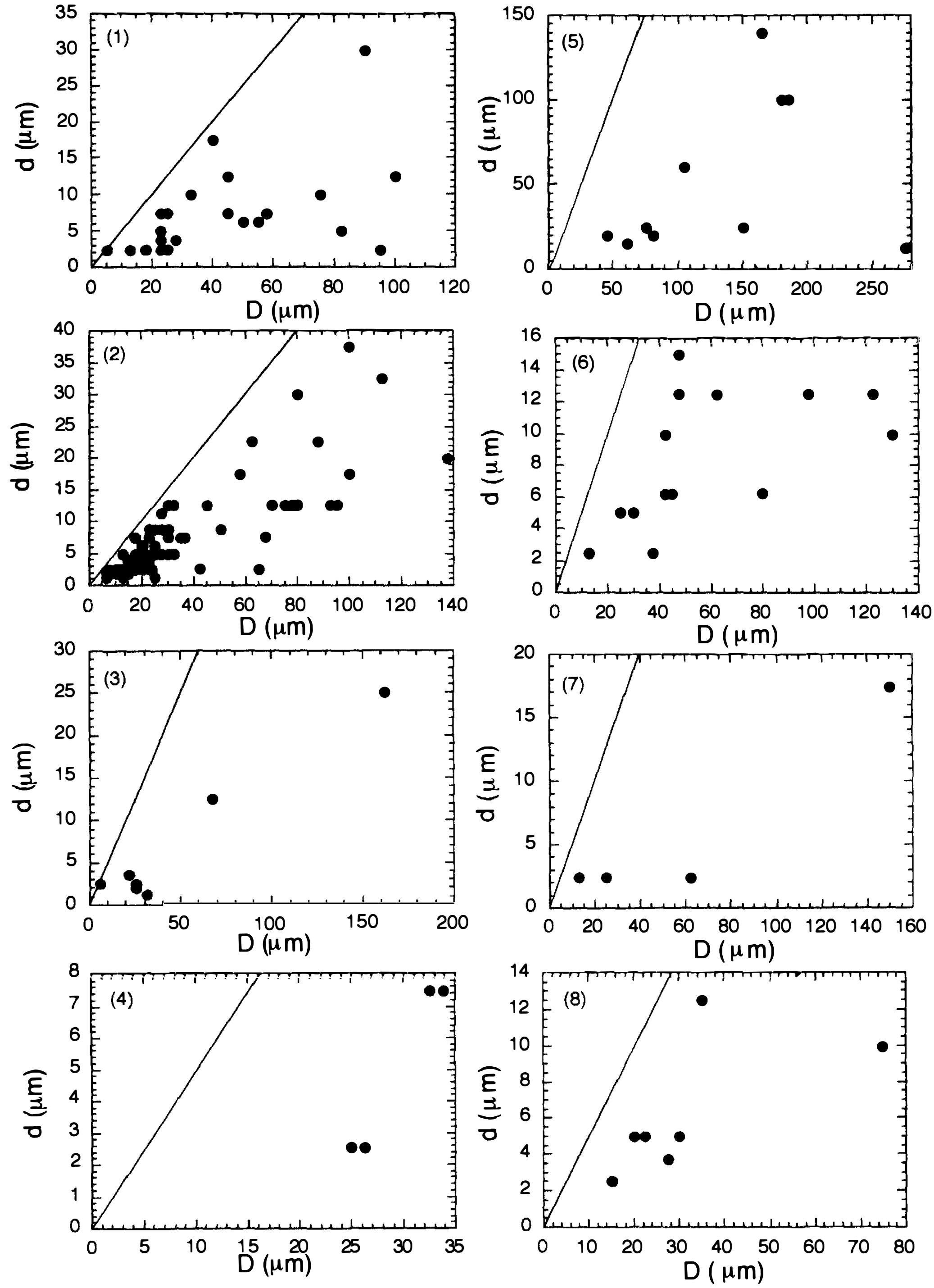

Fig. 2. The relationships between the grain diameter and the rim thickness of rimmed FeNi metals for 22 CO3s. The straight line of each figure shows d = D/2. (1) ALH-77003,89-2. (2) ALH-77307,85-1. (3) Y-791131,51-1. (4) Y-791433,51-1. (5) Y-791717,62-5. (6) Y-791745,51-1. (7) Y-791746,51-1. (8) Y-791748,51-2. (9) Y-794088,51-1. (10) Y-81002,51-1. (11) Y-81020,56. (12) Y-81067,51-1. (13) Y-81068,51-1. (14) Y-82004,51-1. (15) Y-82050,101-2. (16) Y-82094,91-1. (17) Y-8339,51-1. (18) Lance, 50-1. (19) Isna,20-1. (20) Ornans,1105-5. (21) Kainsaz,2486-9. Colony was not measured since opaque minerals were heavily weathered.

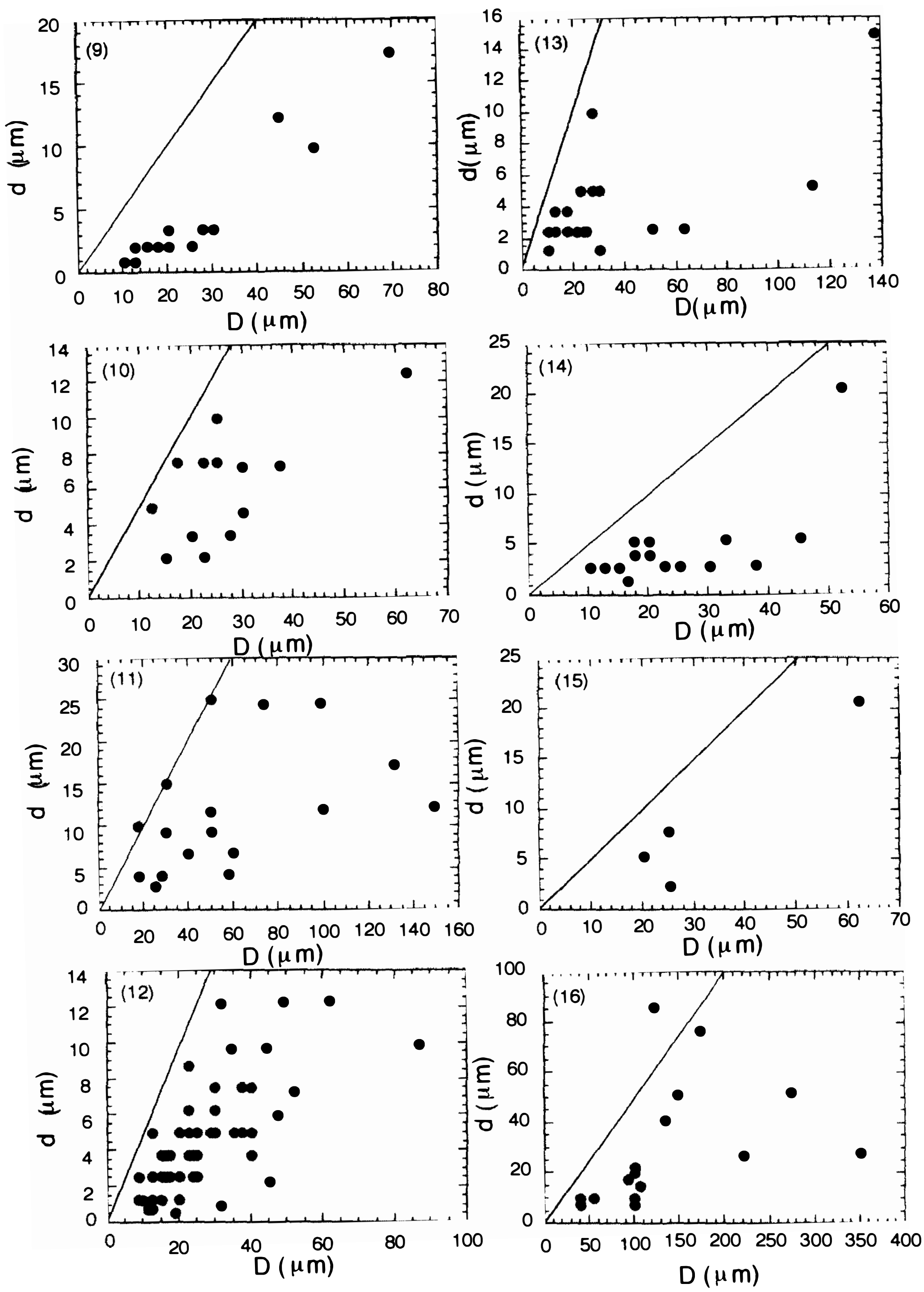

Fig. 2. (continued).

where D_{real} is a sphere diameter and d_{real} is a sphere thickness. The distribution is graphically shown in Fig. 3. The end point shown in Fig. 3 gives (D_{real}, d_{real}). *D-d* distribution in Fig. 2 is clearly different from that of Fig. 3 even if the shape is taken into account. It implies that the real *D* and *d* distributions in CO3s are not three-dimensionally uniform. If we assume that rimmed FeNi metals in CO3s are

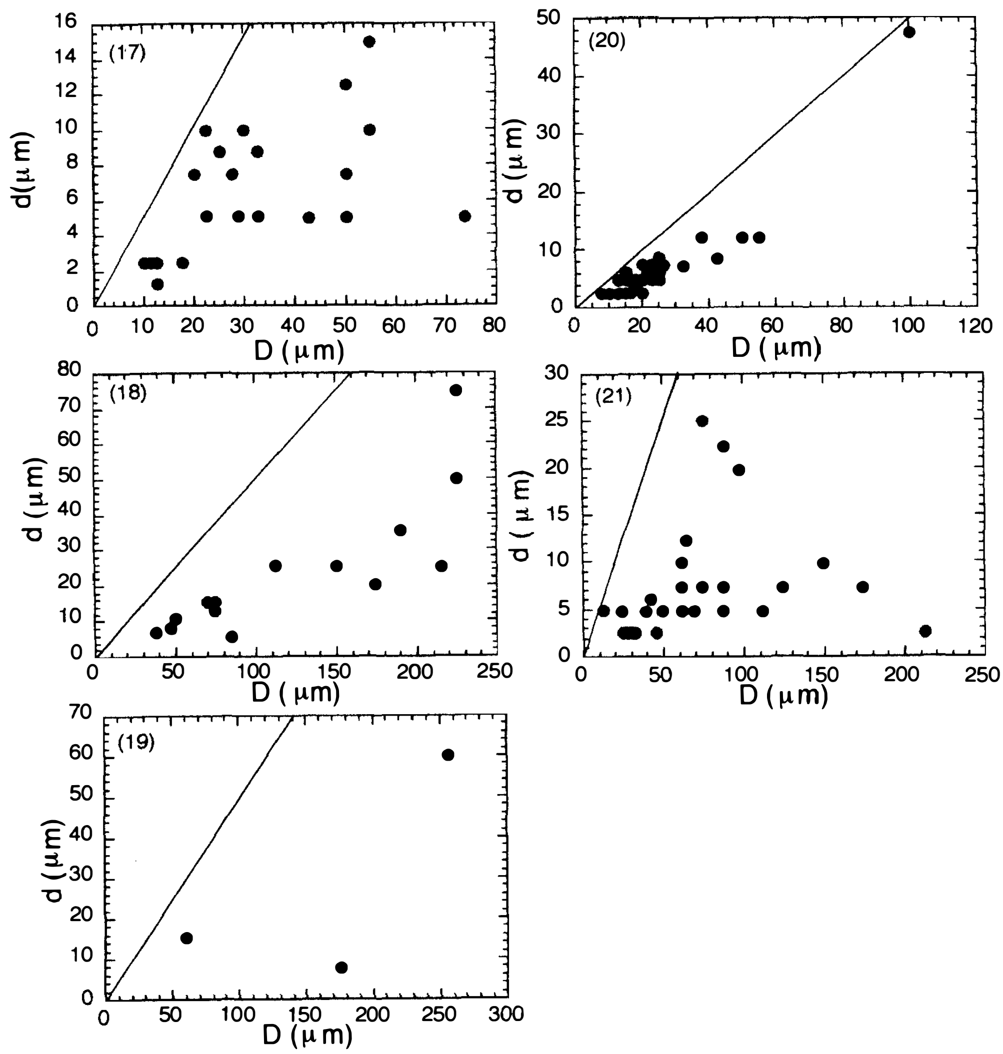

Fig. 2. (continued).

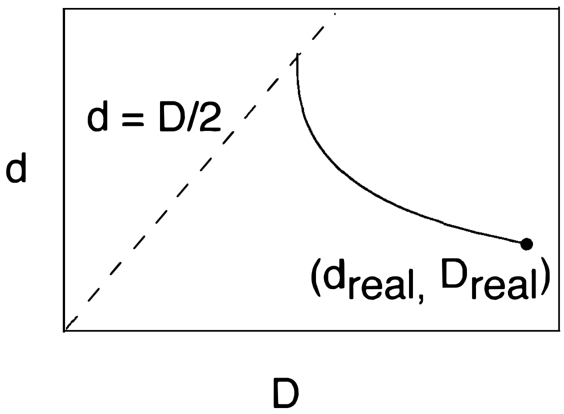

Fig. 3. Schematic distribution of apparent diameter D and rim thickness d in arbitrary cuts through a sphere of diameter (D_{real}) with a constant rim thickness (d_{real}).

spherical and that the rims are uniform in thickness, the *D* and *d* distribution of the obtained data means the assemblages of rimmed FeNi metals with various *D* and *d*. We can interpret the distribution in Fig. 2 into two cases as Fig. 4 in more detail. One interpretation is shown in Fig. 4a. *D* and *d* are distributed with the relation that

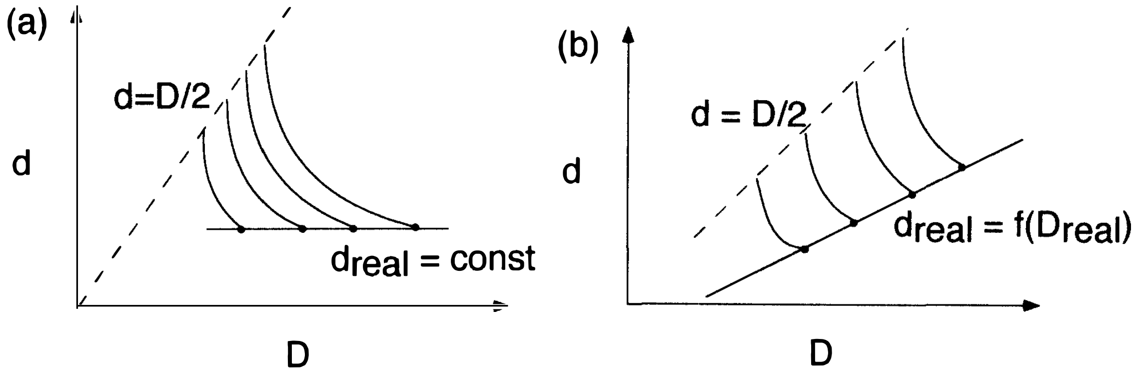

Fig. 4. Possible two interpretations of the D-d distribution. (a) d_{real} is constant irrespective of D. (b) d_{real} is a function of D_{real} with positive slope.

d_{real} is constant irrespective of the grain diameter D. Another is shown in Fig. 4b. This case, D and d are distributed such that D_{real} and d_{real} have a positive correlation. Whether each case is correct can not be judged for all figures since the data points are restricted for each PTS. Thus in the present study, we simply averaged the measured size (D_{mean}) and rim thickness (d_{mean}). In the following discussion, D_{mean} and d_{mean} are used.

4.2. *Compilation of the D and d with the subtype*

We determined the number density of rimmed FeNi metals since it is expected that the number density of these metals is related to the size and thickness distribution. The relationship between the number density and D_{mean} and d_{mean} in Fig. 5a and 5b, respectively, shows that the number density of rimmed metals in each CO3 is lower for a larger grain and for a thicker rim.

The compilation of the diameter and the thickness of rimmed metals with the subtype for each CO3 is shown in Fig. 6a and 6b, respectively. D_{mean} and d_{mean} are not significantly correlated with subtype ($n=21$, $r=0.27$ for D_{mean}; $n=21$, $r=0.15$ for d_{mean}). It has been known that Y-82094 and Lance include fizzed troilite suggesting shock melting (Scott *et al.*, 1992; Imae and Kojima, 2000), this D and d distribution of these meteorites must have been modified by the shock melting. When Y-82094 and Lance are excluded, the correlations become larger ($n=19$, $r=0.52$ for D_{mean}; $n=19$, $r=0.30$ for d_{mean}). The relationship between the subtype and the number density of rimmed metal grains was also shown (Fig. 7). In Fig. 7, the number density decreases with the increase of subtype. Inverse correlation between minimum number density of these metals and subtype is consistent with positive correlation between D_{mean}-d_{mean} and subtype.

4.3. *Implication of the present results*

If magnetite and troilite in rimmed metals should be all produced by a series of thermal metamorphism (3.0 to 3.4), magnetite rimmed metals might be replaced to troilite rimmed metals proceeding by the thermal metamorphism. In this case, troilite rim might occur as outermost rim. However, the observation shows that outermost rim is magnetite and inner rim is troilite (Fig. 1b). Thus the morphology

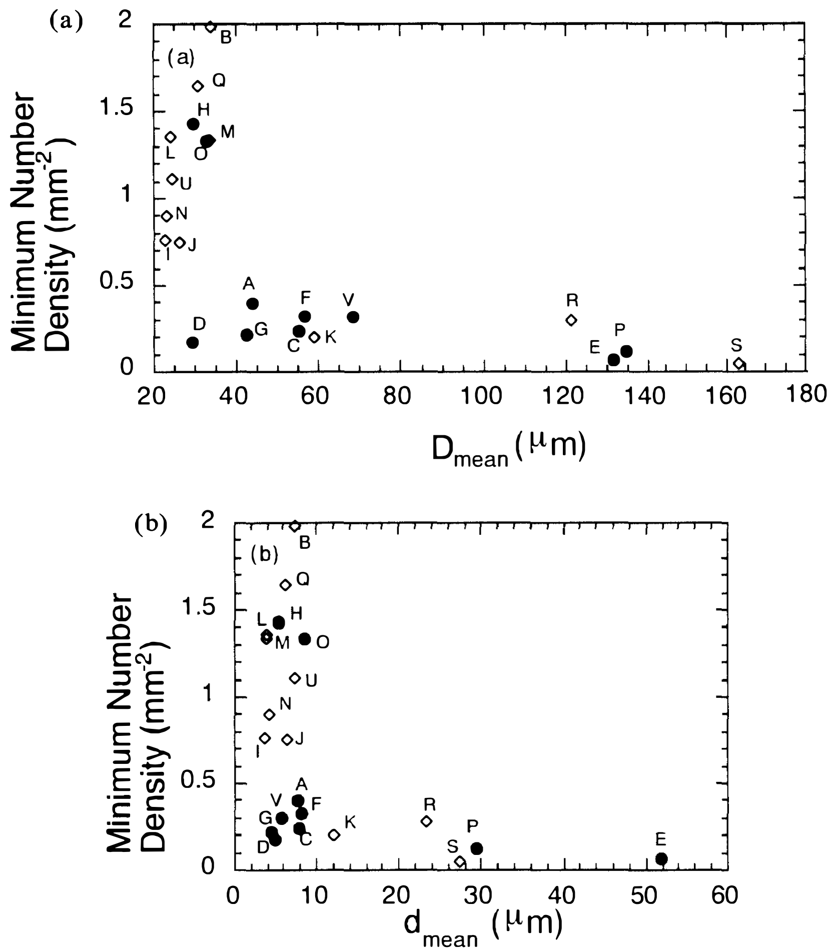

Fig. 5. (a) The relationship between D_{mean} and the minimum number density of rimmed FeNi metal grains. (b) The relationship between d_{mean} and the minimum number density of rimmed FeNi metal grains. Open symbol: magnetite can be observed contained in PTS. Closed symbol: magnetite is not observed in PTS.

of inner troilite and outer magnetite rim cannot be explained by one series of thermal metamorphism determined subtype. The textural variation seen in each subtype could be formed by one of the following ways.

(1) O/S conditions at the time of thermal metamorphism on the parent body were different, that is, O/S was higher for lower subtype, O/S intermediate for intermediate subtype, and O/S lower for higher subtype.

(2) Coexisting rims of magnetite and troilite (Y-81020 and ALH-77307) were pristine. This conclusion obtained in the present study is consistent with previous studies (Shibata, 1996) that ALH-77307 and Y-81020 are least metamorphosed CO3. Oxidation on the parent body formed lower subtype, and sulfide formation on the parent body formed higher subtype.

(3) Some of rimmed metals, especially, magnetite rimmed metals in chondrules which are enclosed in mafic silicates, at lower subtype were formed in the solar nebula. Other rimmed FeNi metals were formed during thermal metamorphism similar to the mechanism of (1).

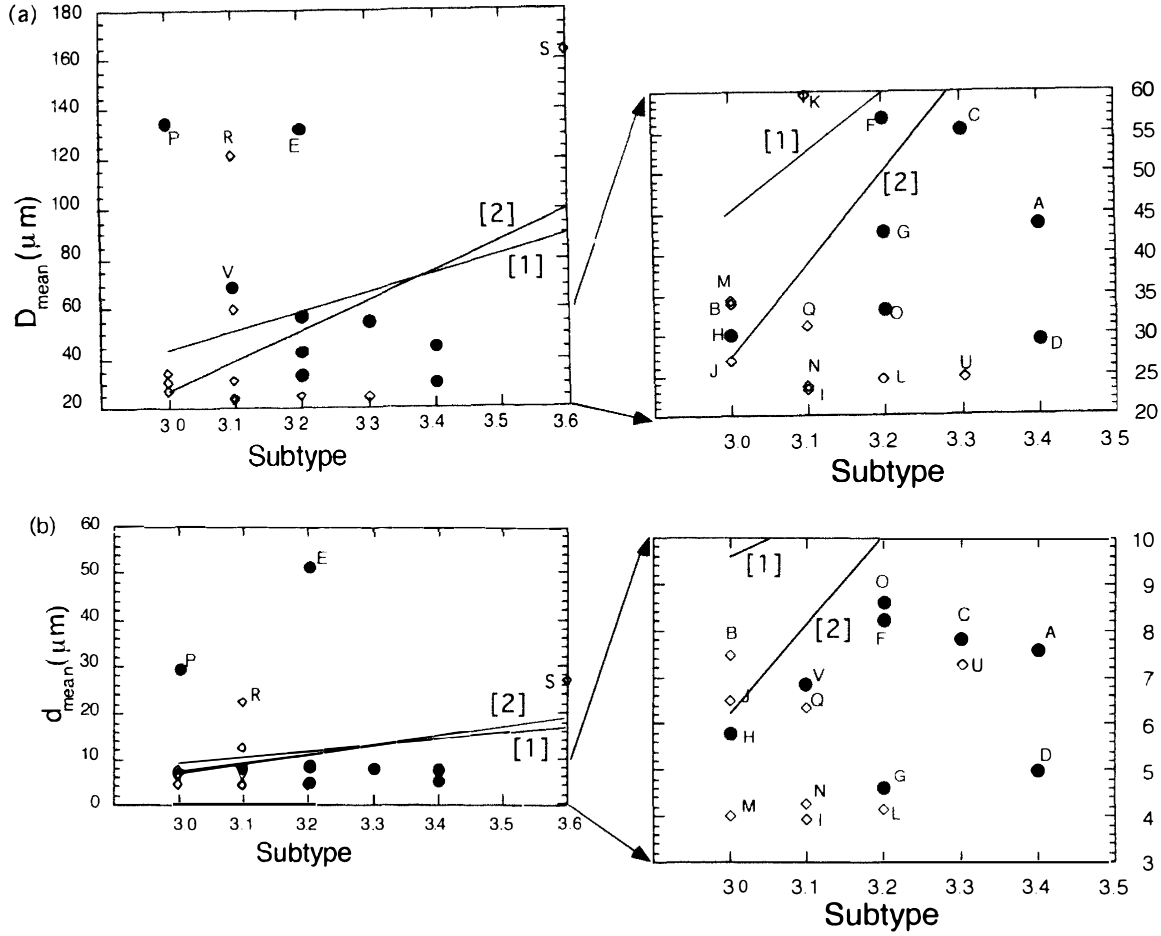

Fig. 6. [1] shows least square lines including all data, and [2] shows square lines except Y-82094 and Lance. Closed symbol: magnetite is not observed in PTS but sulfide is dominant. (a) The relationship between D_{mean} and subtype in CO3 chondrites. $r=0.27$ for [1] and $r=0.52$ for [2]. (b) The relationship between d_{mean} and subtype in CO3 chondrites. Open symbol: magnetite is observed in PTS. $r=0.15$ for [1] and $r=0.30$ for [2].

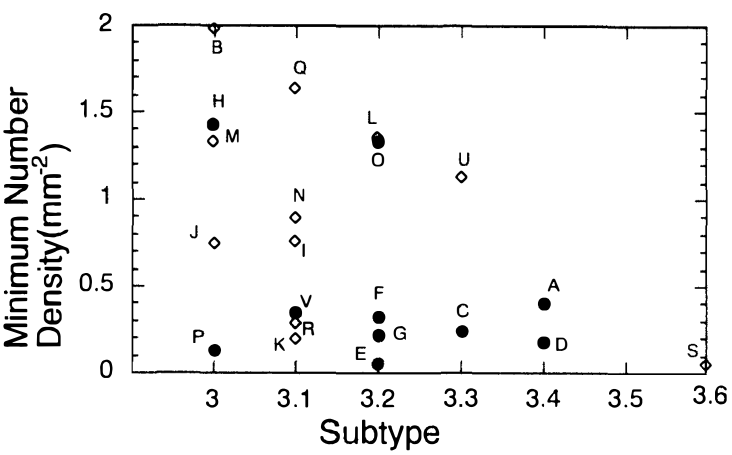

Fig. 7. The relationship between subtype and number density. Open symbol: magnetite is observed in PTS. Closed symbol: magnetite is not observed in PTS.

It is difficult to determine which model is correct. In addition, oxide in Isna might be formed by the hydrothermal metamorphism during the increase of subtype more than 3.4 (Rubin, 1998).

5. Summary

1) Troilite and/or magnetite rimmed FeNi metals commonly occur in 22 CO3 chondrites.

2) Grain size and rim thickness of rimmed metals in a CO3 chondrite are positively correlated. This does not directly mean that the grain size and rim thickness three-dimensionally have a positive correlation.

3) In CO3 chondrites of petrologic subtype less than 3.2, magnetite can be found. Magnetite rimmed metals are abundant and number density of the grain is higher. In chondrites with higher petrologic subtype more than 3.2, magnetite is poor, but troilite is abundant. Troilite rimmed metals are predominant, and number density of the grain is lower. Both the grain size and the rim thickness of these grains are not significantly correlated with subtype.

4) In subtype CO3s less than 3.2, troilite as inner rim and magnetite as outer rim could coexist for some rimmed metals (ALH-77307 and Y-81020). These textural variations of rimmed FeNi metals were not formed by one series of thermal metamorphism.

Acknowledgments

We are grateful to Dr. E. R. D. Scott and an anonymous reviewer for the constructive reviews of the manuscript. We are grateful to Smithsonian Institution for the loan of the PTSs of Ornans and Kainsaz. This research is partially supported by Grant-in-Aid for Scientific Research from the Ministry of Education, Science, Sports and Culture of Japan (No. 07740425).

References

Eisenhour, D. D. (1996): Determing chondrule size distributions from thin-section measurements. Meteorit. Planet. Sci., **31**, 243–248.

Haggerty, S. E. and McMahon, B. M. (1979): Magnetite-sulfide-metal Complexes in the Allende meteorite. Proc. Lunar Planet. Sci. Conf., **10th**, 851–870.

Hughes, D. W. (1978): A disaggregation and thin section analysis of the size and mass distribution of the chondrules in the Bjurbole and Chainpur meteorites. Earth Planet. Sci. Lett., **38**, 391–400.

Imae, N. (1994): Direct evidence of sulfidation of metallic grain in chondrites. Proc. Jpn. Acad., **70**, Ser. B, 133–137.

Imae, N. and Kojima, H. (2000): Sulfide textures of a unique CO3-chondrite (Y-82094) and its petrogenesis. Antarct. Meteorite Res., **13**, 55–64.

McSween, H. Y., Jr. (1977): Carbonaceous chondrites of the Ornans type: a metamorphic sequence. Geochim. Cosmochim. Acta, **41**, 477–491.

Kojima, T., Yada, S. and Tomeoka, K. (1995): Ca-Al-rich inclusions in three antarctic CO3 chondrites, Yamato-81020 and Yamato-790992: Record of low-temperature alteration. Proc. NIPR Symp. Antarct. Meteorites, **8**, 79–96.

Krot, A. N., Zolensky, M. E., Wasson, J. T., Scott, E. R. D., Keil, K. and Ohsumi, K. (1997): Carbide-mangetite assemblages in type-3 ordinary chondrites. Geochim. Cosmochim. Acta, **61**, 219–237.

Krot, A. N. and Todd, C. S. (1998): Metal-carbide-magnetite-fayalite association in a Bali-like clast in the reduced CV3 chondrite breccia Vigarano. Meteorit. Planet. Sci., **33**, Suppl., 89.

Lauretta, D. S., Kremser, D. T. and Fegley, B., Jr. (1996a): A comparative study of experimental and meteoritic metal-sulfide assemblages. Proc. NIPR Symp. Antarct. Meteorites, **9**, 97–110.

Lauretta, D. S., Kremser, D. T. and Fegley, B., Jr. (1996b): The rate of iron sulfide formation in the solar nebula. Icarus, **122**, 288–315.

Lauretta, D. S., Lodders, K., Fegley, B., Jr. and Kremser, D. T. (1997): The origin of sulfide-rimmed metal grains in ordinary chondrites. Earth Planet. Sci. Lett., **151**, 289–301.

Rubin, A. E. (1989): Size-frequency distributions of chondrules in CO3 chondrites. Meteoritics, **24**, 179–189.

Rubin, A. E. (1991): Euhedral awaruite in the Allende meteorite: Implications for the origin of awaruite- and magnetite-bearing nodules in CV3 chondrites. Am. Mineral., **76**, 1356–1362.

Rubin, A. E. (1998): Correlated petrologic and geochemical chracteristics of CO3 chondrites. Meteorit. Planet. Sci., **33**, 385–391.

Rubin, A. E., Sailer, A. L. and Wasson, J. T. (1999): Troilite in the chondrites of type-3 ordinary chondrites: Implications for chondrule formation. Geochim. Cosmochim. Acta, **63**, 2281–2298.

Scott, E. R. D. and Jones, R. H. (1990): Disentangling nebular and Asteroidal features of CO3 carbonaceous chondrite meteorites. Geochim. Cosmochim. Acta, **54**, 2485–2502.

Scott, E. R. D., Keil, K. and Stofler, D. (1992): Shock metamorphism of carbonaceous chondrites. Geochim. Cosmochim. Acta, **56**, 4281–4293.

Sears, D. W. G., Batchelor, J. D., Lu, J. and Keck, D. (1991): Metamorphism of CO and CO-like chondrites and comparisons with type 3 ordinary chondrites. Proc. NIPR Symp. Antarct. Meteorites, **4**, 319–343.

Shibata, Y. (1996): Opaque minerals in Antarctic CO3 carbonaceous chondrites, Yamato-74135, -790992, -81020, -81025, -82050 and Allan Hills-77307. Proc. NIPR Symp. Antarct. Meteorites, **9**, 79–96.

Shibata, Y. and Matsueda, H. (1994): Chemical composition of Fe-Ni metal and phosphate minerals in Yamato-82094 carbonaceous chondrite. Proc. NIPR Symp. Antarct. Meteorites, **7**, 110–124.

(Received September 6, 1999; Revised manuscript received January 18, 2000)